International Journal of Microwave and Wireless Technologies

cambridge.org/mrf

A wideband dielectric resonator antenna with switchable diversity patterns

Ahmad Abdalrazik[1], Adel B. Abdel-Rahman[1,2], Ahmed Allam[1] and Mohammed Abo-Zahhad[1,3]

[1]ECE Department, Egypt-Japan University of Science and Technology, Alexandria 21934, Egypt; [2]Electrical Engineering Department, Faculty of Engineering, South Valley University, Qena 83523, Egypt and [3]Electrical and Electronics Engineering Department, Faculty of Engineering, Assiut University, Assiut, Egypt

Research Paper

Cite this article: Abdalrazik A, Abdel-Rahman AB, Allam A, Abo-Zahhad M (2020). A wideband dielectric resonator antenna with switchable diversity patterns. *International Journal of Microwave and Wireless Technologies* **12**, 339–344. https://doi.org/10.1017/S1759078719001466

Received: 25 May 2019
Revised: 28 October 2019
Accepted: 29 October 2019
First published online: 22 November 2019

Keywords:
Dielectric resonator antenna; diversity; wideband

Author for correspondence:
Ahmad Abdalrazik, E-mail: ahmad.abdalrazik@ejust.edu.eg

Abstract

In this paper, a reduced-size dielectric resonator antenna with switchable diversity patterns is proposed. Ring- and linear-shaped slots are etched in the ground plane of the antenna so as to generate two modes $TE^x_{\delta 11}$ and $TE^x_{\delta 12}$ at a center frequency of 19 GHz. Moreover, two groups of PIN diodes are integrated into these slots to short one group of slots, and let the other group generates the required mode. Thus, the antenna is able to generate two switchable patterns with an envelope correlation coefficient of 0.4. Furthermore, the antenna size is reduced to half of its original size by placing a copper sheet over certain plane of the antenna structure. The antenna achieves wide bandwidths of 17.6–20.9 GHz (17.1%) and 18.3–21.6 GHz (13.8%) in cases of exciting $TE^x_{\delta 11}$ and $TE^x_{\delta 12}$ modes, respectively. The antenna also attainsa high gain of 7.1 and 3.2 dB at the center frequency.

Introduction

The dielectric resonator antenna (DRA) was shown to be an efficient radiator that offers a compact size, high radiation efficiency, and wide impedance bandwidth. Moreover, it provides several design degrees of freedom, which enhances its performance and enables it to serve as an multifunctional device. For instance, the dimensions of the DRA could be tuned to excite multiple modes to create amultiple-input multiple-output (MIMO) antenna [1,2]. Also, the DRA has been used to generate circularly polarized wave by exciting two orthogonal modes inside it [3,4]. Furthermore, the DRA could serve as a frequency-reconfigurable antenna where switches are used to select multiple frequency bands [5]. In the aforementioned work, the authors proposed four identical rectangular dielectric resonator blocks with a permittivity of 10. PIN diode switches are integrated into the feed lines between the dielectric resonator blocks to generate four operating bands, where different modes are excited inside the DRAs to generate the four operating bands.

Moreover, generating multiple modes inside DRAs are used to create antennas with polarization diversity patterns [6–9]. In [6], cylindrical DRA with a top-loaded Alford loop is investigated. Two ports are utilized to excite two different modes inside the DRA, such that the two modes radiate like vertical and horizontal magnetic dipoles. As the electric field polarizations of the two modes are perpendicular to each other, the two ports exciting these two modes are able to receive signals independently, and considered as two diversity branches. In [7], another DRA structure was proposed, such that orthogonal modes were excited in a single dielectric resonator structure. The feeding network of the antenna has been designed such that two orthogonal modes TE^x_{111} and TE^y_{111} are excited through the two ports of the antenna, which are considered as receive diversity branches.

The DRA was also shown to be able to create recieve/transmit diversity patterns in [10], where a cylindrical DRA with switchable beams was proposed. An annular slot was placed underneath the DRA, with eight switches soldered across it. By turning on one of the eight PIN diodes, the proposed antenna can rotate the beam to the opposite direction of the switch. The bandwidth of the antenna is 3.64%. Other several pattern diversity antennas were also studied in the literature [11–16]. In [11], a hybrid antenna with switchable diversity patterns was proposed. The hybrid antenna consists of several parasitic elements that are closely-placed around a driven antenna, where each parasitic element is composed of a printed dipole with a PIN diode. Using different combinations of PIN diode ON/OFF states, the radiation pattern can be switched toward different directions. The polarization of the antenna is controlled by changing the feeding point of the antenna. The bandwidths of the antenna ports are 0.06, 0.08, and 0.04%. In [12], two patch antennas were proposed to radiate multiple patterns as desired for both on- and off-body applications. An omni-azimuthal radiation pattern directed along the body and a broadside radiation directed away from the body respectively. This was achieved by exciting the fundamental TM_{11} mode ina classical circular patch antenna for off-body radiation and the TM_{01} mode in another circular patch antenna. However, the antenna fractional BW was only 0.036 and 0.06%. In [16], a MIMO system that consists of a chamfered edge square patch antenna with an offset feed and two printed dipole antennas, was proposed. Three diversity patterns were generated with less than −18 dB coupling. The antenna fractional BW was only 16.2, 16.2, and 4.14%.

In this paper, a reduced sized DRA that generates two switchable diversity patterns is proposed. The two modes $TE^x_{\delta 11}$ and $TE^x_{\delta 12}$ are excited through ground slots, where the electric field distributions of the two modes are symmetrical over the *xz* plane. Thus, a perfect electric conductor is used to reduce the antenna size to half. PIN diodes are placed over the slots so as to allow only one slot to generate a mode inside the DRA, which simplifies the input structure of the antenna. The envelope correlation coefficient (ECC) is found to be 0.4 which is an acceptable value [17]. Compared to previous publications [11–16], this simple and novel design consists of only a single element DRA, and is fed by only one port while being able to create two diversity patterns. Moreover, the size of the proposed DRA antenna with switchable patterns is reduced to half of its original size through placing a copper sheet over the DRA. Furthermore, the antenna achieves wide fractional bandwidths of 17.1, and 13.8% in cases of exciting $TE^x_{\delta 11}$ and $TE^x_{\delta 12}$ modes, respectively. The antenna also attains a high gain of 7.1 and 3.2 dB at the center frequency although its size is reduced to half of the original size.

The proposed DRA design

Antenna design

The antenna consists of a rectangular DRA with dimensions of 7.2 mm × 8.1 mm × 1.9 mm as shown in Fig. 1. Linear and ring slots are placed on the ground plane to generate two switchable modes inside the DRA. Also, PIN diodes are placed over the slots so as to allow only one of the slots to couple power inside the DRA. The DRA material is Rogers 3010 with $\epsilon_r = 10.1$. The feeding structure is a microstrip antenna with dielectric made from Rogers 5880 with $\epsilon_r = 2.2$. As will be explained in the next subsection, the symmetry of the antenna enables to place a copper sheet upon one side of the DRA, which serves as a mirror for internal fields of the DRA, and reduces the antenna size to half, as shown in Fig. 2.

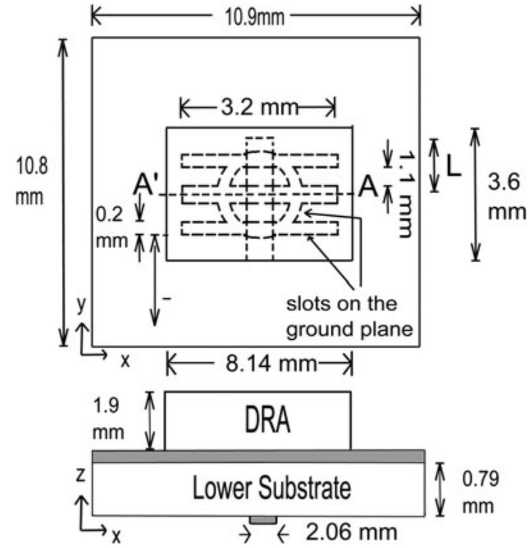

Fig. 1. Antenna geometry of the proposed DRA.

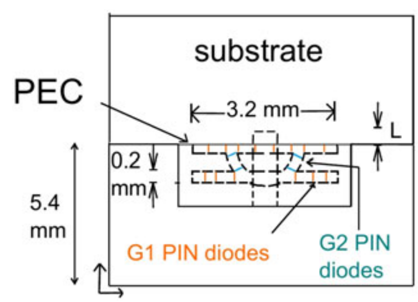

Fig. 2. Proposed antenna's size is reduced to half. Two groups of diodes G1 and G2 are placed over the slots. The space between each two diodes is 0.5 mm.

Modes excitation analysis

By choosing appropriate dimensions for the proposed DRA, the two modes $TE^x_{\delta 11}$ and $TE^x_{\delta 12}$ could be excited inside it. Based on the waveguide model of the DRA [18], a resonance frequency of an TE^x mode is related to the DRA's dimensions according to the following transcendental equation

$$k_x \tan(k_x d/2) = \sqrt{(\epsilon - 1)k_0^2 - k_x^2} \quad (1)$$

where $k_0^2 = (k_x^2 + k_y^2 + k_z^2)/\epsilon$, $k_0 = 2\pi f_0/c$, $k_x = \delta\pi/d$, and $k_y = n\pi/w$, $k_z = p\pi/b$; f_0 is the mode resonance frequency and *c* is the speed of light; *d*, *w* and *b* are the DRA dimensions in the *x*, *y*, and *z* directions, respectively; *n* and *p* are positive integers, and δ is a positive fraction of unity.

Thus, a DRA with dimensions of 7.2 mm × 8.1 mm × 1.9 mm generates the two modes $TE^x_{\delta 11}$ and $TE^x_{\delta 12}$ with resonance frequencies of 19 and 22 GHz, respectively. To verify this, the previous transcendental equation (1) is rewritten as

$$D_{TE^x}(f) = k_x \tan(k_x d/2) - \sqrt{(\epsilon - 1)k_0^2 - k_x^2} \quad (2)$$

where by plotting the $D_{TE^x}(f)$ function as shown in Fig. 3, every zero-crossing represents a resonance frequency for a generated mode. Thus, the modes $TE^x_{\delta 11}$ and $TE^x_{\delta 12}$ are obtained at frequencies of 19 and 22 GHz, respectively. Furthermore, the proposed antenna structure is simulated using CST Microwave Studio commercial software, where simulated and theoretical electric field distributions for modes $TE^x_{\delta 11}$ and $TE^x_{\delta 12}$ at frequencies of 19and 22 GHz are shown in Fig. 4. It is noted that the simulated electric field distributions (Figs. 4(a) and 4(c)) are very close to the theoretical field distributions of modes $TE^x_{\delta 11}$ and $TE^x_{\delta 12}$ (Figs. 4(b) and 4(d)). Also, it is noted that simulated modes $TE^x_{\delta 11}$ and $TE^x_{\delta 12}$ at frequencies of 19 and 22 GHz, respectively, agree with the theoretical resonance frequencies obtained from Fig. 3.

Interestingly, it is seen from Fig. 4 that the electric field vectors of both modes $TE^x_{\delta 11}$ and $TE^x_{\delta 12}$ are normal to the plane *AA*′. Thus, a copper sheet can be placed over the plane *AA*′, while field distributions of both modes are not effected. This copper sheet serves as a mirror for fields generated inside the DRA,

https://doi.org/10.1017/S1759078719001466 Published online by Cambridge University Press

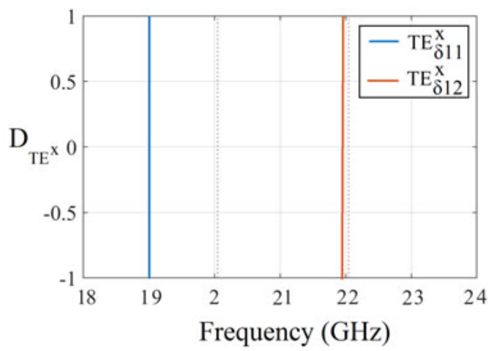

Fig. 3. Plot of *D* function. The modes $TE^x_{\delta 11}$ and $TE^x_{\delta 12}$ are obtained at frequencies of 19 and 22 GHz.

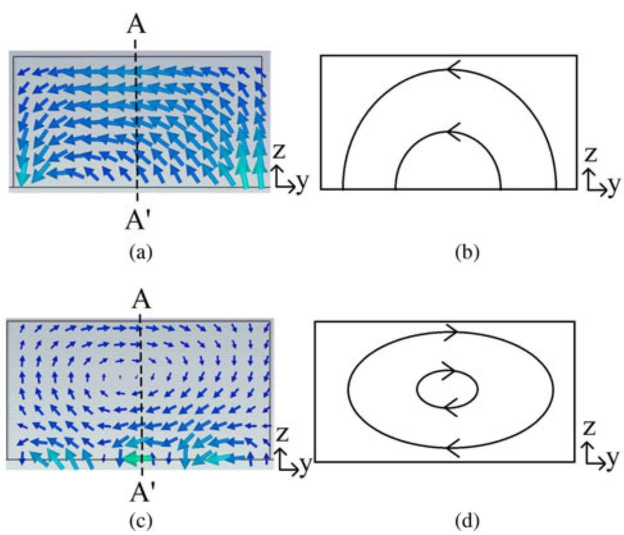

Fig. 4. (a) Simulated electric field distribution of $TE^x_{\delta 11}$ in the *yz* cross section of the DRA at a frequency of 19 GHz. (b) Theoretical electric field distribution of $TE^x_{\delta 11}$ in the *yz* cross section of the DRA, (c) simulated electric field distribution of $TE^x_{\delta 12}$ in the *yz* cross section of the DRA at a frequency of 22 GHz, and (d) theoretical electric field distribution of $TE^x_{\delta 12}$ in the *yz* cross section of the DRA.

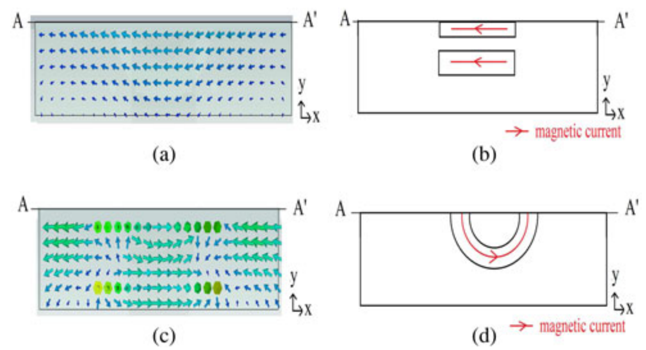

Fig. 5. (a) Simulated magnetic field distribution of $TE^x_{\delta 11}$ in the ground plane at a frequency of 19 GHz, (b) equivalent magnetic current excited in linear slots when G2 are turned off, (c) simulated magnetic field distribution of $TE^x_{\delta 12}$ in the ground plane at a frequency 22 GHz, and (d) equivalent magnetic current excited in circular slots when G1 are turned off.

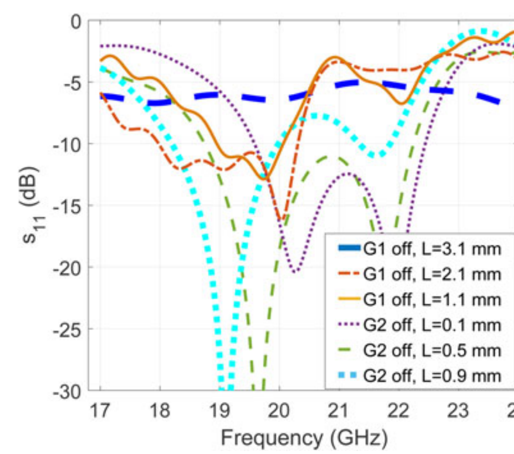

Fig. 6. Effect of stub length changes on the S_{11} value of the proposed antenna for the two cases where G1 and G2 are off.

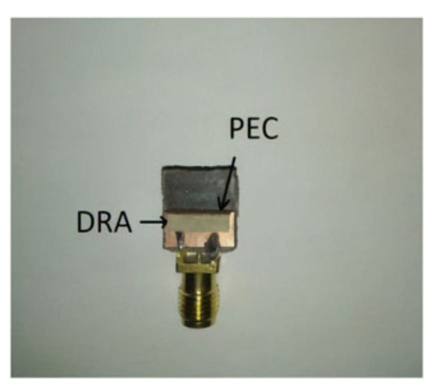

Fig. 7. Prototype of the proposed antenna.

and keeps the resonance frequencies of the modes unchanged, while reducing the antenna size to half as shown in Fig. 2.

Two groups of slots are etched into the ground plane to couple power from the microstrip antenna to the DRA. The first group consists of linear slots that generate linear equivalent magnetic current, as shown in Fig. 5(b); and the second group consists of a circular slot that generates circular equivalent magnetic current as shown in Fig. 5(d). PIN diodes are placed over the slots of the antenna, where the groups of PIN diodes over the linear slot are referred to as G1, and those over the ring slot are referred to as G2.

The magnetic field distributions for the modes $TE^x_{\delta 11}$ and $TE^x_{\delta 12}$ are shown in Figs. 5(a) and 5(c), respectively. When G1 diodes are turned off and G2 diodes are turned on, magnetic currents are excited through the linear slots and couple power to the DRA (Fig. 5(b)), which generates the mode $TE^x_{\delta 11}$. On the other hand, when G2 diodes are turned off and G1 diodes are turned on, magnetic currents are excited through the ring slot and couple power to the DRA (Fig. 5(d)), which generates the mode $TE^x_{\delta 12}$. This technique simplifies the feeding structure of the antenna since only one feeding line is needed to excite the antenna. The two modes excited by these slot groups generate two switchable patterns with low ECC as it will be shown in the next section, which creates diversity patterns for the proposed antenna.

Furthermore, the stub length affects the matching of the antenna in the two cases of switch states. S_{11} of the proposed antenna for the two cases of the switch states is shown in Fig. 6. The simulation is done using CST Microwave Studio commercial software. Clearly, the optimum value for the stub length is

https://doi.org/10.1017/S1759078719001466 Published online by Cambridge University Press

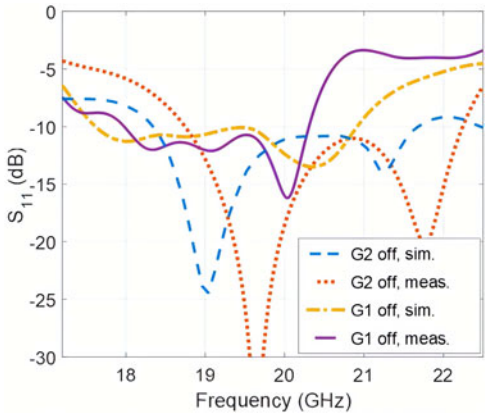

Fig. 8. S_{11} value for the proposed antenna at the optimized lengths.

Table 1. Comparison of fractional bandwidth for the proposed antenna and previous designs.

Ref.	Fractional bandwidth (%)
Masood et al. [12]	0.03, 0.06
Gu et al. [11]	0.08, 0.06, 0.04
Saurav et al. [19]	2.7, 11.4, 11.88
Sharma et al. [16]	16.2, 16.2, 4.14
Malik et al. [20]	0.08
Proposed design	17.1, 13.8

2.4 mm when G2 is turned on, while the optimum value for the stub length is 1.4 mm when G1 is turned on. A PIN diode is placed over the stub to switch its length between 2.4 and 1.4 mm.

Simulation and experimental results

The proposed antenna is simulated and fabricated as shown Fig. 7; measurements are taken using a Vector Network Analyzer. Simulated and measured *S*-parameters of the proposed antenna are shown in Fig. 8. The simulated bandwidths are 17.6–20.9 GHz (17.1%), and 18.3–21.6 GHz (13.8%) in cases of turning off G1 diodes and G2 diodes, respectively. The measured bandwidths are 18–20.3 GHz (12%) and 18.8–22.2 GHz (16.6%) in cases of turning off G1 diodes and G2 diodes, respectively. Thus, the proposed antenna attains very good bandwidth compared to previous designs, as shown in Table 1. Also, the two patterns generated by the antenna are shown in Fig. 9, where the first pattern is generated when G1 diodes are turned off and the second pattern is generated when G2 diodes are turned off. It is noted that the gains are 7.1 and 3.2 dB, respectively, and both beam patterns are in the broadside direction. Moreover, the gain over frequency is shown in Fig. 10. It is noted that the gain ranges from 7 to 3 dB over the operating band.

Finally, to calculate the correlation coefficient between the two patterns, we use [16]

$$\rho = \frac{\int_v \beta^1 . \beta^2 dv}{\sqrt{\int_v \beta^1 dv \int_v \beta^2 dv}} \quad (3)$$

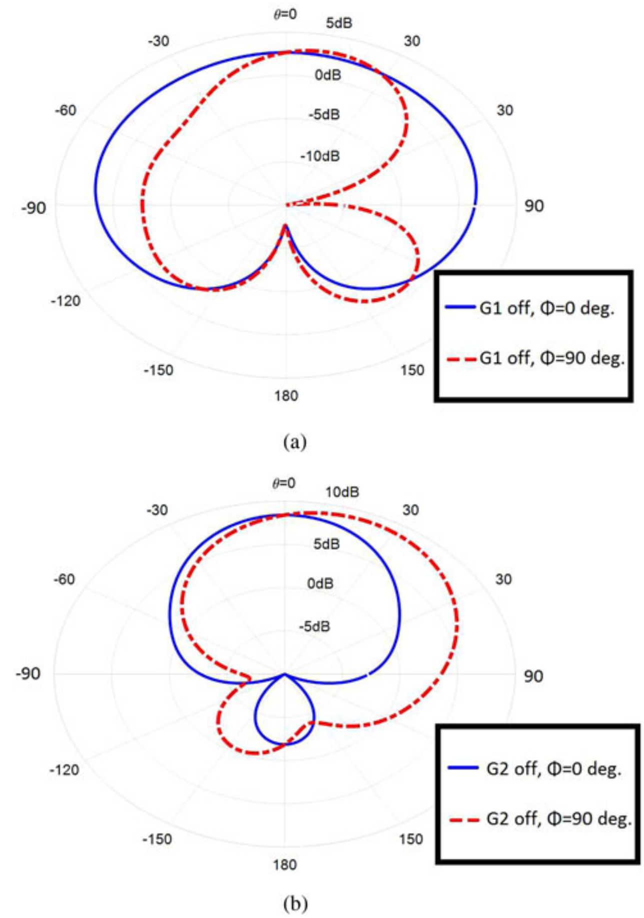

Fig. 9. Cut planes of the power patterns of the proposed antennas for the two cases where (a) G1 diodes are off and (b) G2 didoes are off.

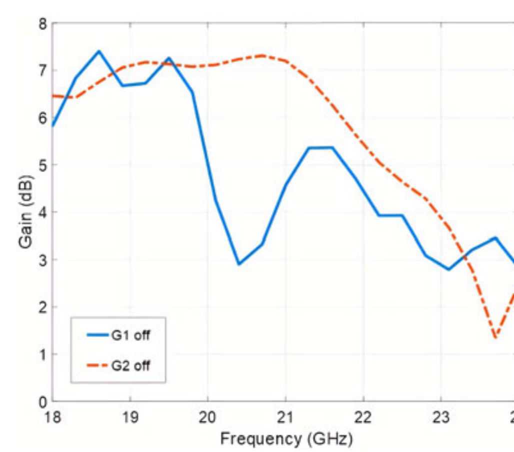

Fig. 10. Gain frequency response plot for the proposed antenna.

where β^i is the *i*th power pattern. The value of ρ is 0.4 which is less than the maximum acceptable limit of 0.7 [17].

Conclusion

A wideband DRA with switchable diversity patterns is proposed in this paper. Ring- and linear-shaped slots are placed on the

https://doi.org/10.1017/S1759078719001466 Published online by Cambridge University Press

ground to generate two modes $TE^x_{\delta 11}$ and $TE^x_{\delta 12}$ inside the DRA. Also, PIN diodes are placed over these slots such that only one slot couples power to the DRA, and the corresponding pattern is generated. The ECC between the two switchable patterns is calculated and found to be low. The simulated bandwidths are 17.6–20.9 GHz (17.1%) and 18.3–21.6 GHz (13.8%) in cases of exciting $TE^x_{\delta 11}$ and $TE^x_{\delta 12}$ modes, respectively. The measured bandwidths are 18–20.3 GHz (12%) and 18.8–22.2 GHz (16.6%) in cases of exciting $TE^x_{\delta 11}$ and $TE^x_{\delta 12}$ modes, respectively. Moreover, compared to previous publications [11–16], this simple and novel design consists of only a single element DRA, and is fed by only one port while being able to create two diversity patterns. Furthermore, the antenna size is reduced to half by placing a perfect electric conductor over a symmetry plane of the antenna structure. This reduction in the DRA size saves space that could be utilized in a future design to add a second reduced-sized DRA on the same substrate, which forms an antenna array. Also, the antenna attainsa high gain of 7.1 and 3.2 dB at the center frequency, despite its size reduction to half of the original size.

References

1. **Roslan SF, Kamarudin MR, Khalily M and Jamaluddin MH** (2014) An MIMO rectangular dielectric resonator antenna for 4G applications. *IEEE Antennas and Wireless Propagation Letters*, **13**, 321–324.
2. **Abdalrazik A, El-Hameed AS and Abdel-Rahman AB** (2017) A three-port MIMO dielectric resonator antenna using decoupled modes. *IEEE Antennas and Wireless Propagation Letters*, **16**, 3104–3107.
3. **Chen Z and Wong H** (2018) Liquid dielectric resonator antenna with circular polarization reconfigurability. *IEEE Transactions on Antennas and Propagation*, **66**, 444–449.
4. **Zou L and Fumeaux C** (2011) A cross-shaped dielectric resonator antenna for multifunction and polarization diversity applications. *IEEE Antennas and Wireless Propagation Letters*, **10**, 742–745.
5. **Danesh S, Rahim SK, Abedian M and Hamid MR** (2015) A compact frequency-reconfigurable dielectric resonator antenna for LTE/WWAN and WLAN applications. *IEEE Antennas and Wireless Propagation Letters*, **14**, 486–489.
6. **Li WW and Leung KW** (2013) Omnidirectional circularly polarized dielectric resonator antenna with top-loaded Alford loop for pattern diversity design. *IEEE Transactions on Antennas and Propagation*, **61**, 4246–4256.
7. **Chen Z, Shoaib I, Yao Y, Yu J, Chen X and Parini CG** (2016) Pattern-reconfigurable dual-polarized dielectric resonator antenna. *IEEE Antennas and Wireless Propagation Letters*, **15**, 1273–1276.
8. **Saleem MK, Alkanhal MA and Sheta AF** (2016) Switch beam dielectric resonator antenna array with four reconfigurable radiation patterns. *Microwave and Optical Technology Letters*, **58**, 86–92.
9. **Sun Y and Leung KW** (2015) Wideband rectangular dielectric resonator antenna with polarization diversity. *2015 International Workshop on Electromagnetics: Applications and Student Innovation Competition (iWEM)*, 2015 November 16, pp. 1–2. IEEE.
10. **Zhong L, Hong JS and Zhou HC** (2016) A novel pattern-reconfigurable cylindrical dielectric resonator antenna with enhanced gain. *IEEE Antennas and Wireless Propagation Letters*, **15**, 1253–1256.
11. **Gu C, Gao S, Liu H, Luo Q, Loh TH, Sobhy M, Li J, Wei G, Xu J, Qin F and Sanz-Izquierdo B** (2015) Compact smart antenna with electronic beam-switching and reconfigurable polarizations. *IEEE Transactions on Antennas and Propagation*, **63**, 5325–5333.
12. **Masood R, Person C and Sauleau R** (2017) A dual-mode, dual-port pattern diversity antenna for 2.45-GHz WBAN. *IEEE Antennas and Wireless Propagation Letters*, **16**, 1064–1067.
13. **Zhang Y, Wei K, Zhang Z, Li Y and Feng Z** (2015) A compact dual-mode metamaterial-based loop antenna for pattern diversity. *IEEE Antennas and Wireless Propagation Letters*, **14**, 394–397.
14. **Mak KM, Lai HW, Luk KM and Ho KL** (2017) Polarization reconfigurable circular patch antenna with a C-shaped. *IEEE Transactions on Antennas and Propagation*, **65**, 1388–1392.
15. **Chacko BP, Augustin G and Denidni TA** (2015) Electronically reconfigurable uniplanar antenna with polarization diversity for cognitive radio applications. *IEEE Antennas and Wireless Propagation Letters*, **14**, 213–216.
16. **Sharma Y, Sarkar D, Saurav K and Srivastava KV** (2017) Three-element MIMO antenna system with pattern and polarization diversity for WLAN applications. *IEEE Antennas and Wireless Propagation Letters*, **16**, 1163–1166.
17. **Vaughan RG and Andersen JB** (1987) Antenna diversity in mobile communications. *IEEE Transactions on Vehicular Technology*, **36**, 149–172.
18. **Aldo P** (2007) *Dielectric Resonator Antennas Handbook*, Bostonk, London: Artech House.
19. **Saurav K, Mallat NK and Antar YM** (2018) A three-port polarization and pattern diversity ring antenna. *IEEE Antennas and Wireless Propagation Letters*, **17**, 1324–1328.
20. **Malik J, Nagpal D and Kartikeyan MV** (2016) MIMO antenna with omnidirectional pattern diversity. *Electronics Letters*, **52**, 102–104.

Ahmad Abdalrazik received his B.Sc. degree in Electrical Engineering from Port Said University, Egypt in 2012. He received his M.Sc. degree from the same university in 2016. Currently, he is a Ph.D. student at Egypt-Japan University of Science and Technology (E-JUST), Egypt since 2017. His research interests include antenna design, microwave devices, wave propagation modeling, metamaterial, and optimization.

Adel B. Abdel-Rahman is currently a Professor at the Department of Electronics and Communications Engineering, Egypt-Japan University of Science and Technology, Alexandria, Egypt. He received his B.S. and M.S. in Electrical Engineering, Communication, and Electronics from Assiut University, Egypt, and his Dr.-Ing. degree in Communication Engineering from Otto von Guericke University, Germany in 2005. Since October 2006, he has been an Assistant Professor at the Electrical Engineering Department, South Valley University, Qena, Egypt. He has published more than 120 refereed journal and conference papers and has two patents. He was the Executive Director for Information and Communication Technology, South Valley University, from 2010-2012. Since October 2012, he joined the School of Electronics, Communications and Computer Engineering, Egypt-Japan University of Science and Technology (E-JUST), Alexandria, Egypt, and has been the Dean of the Faculty of Computers and Information, South Valley University from 2016-2018. His research interests include the design and analysis of antennas, filters, millimeter-wave devices, WPT, and metamaterials and their application in wireless communication, as well as optimization techniques with applications to microwave devices and antenna arrays.

Ahmed Allam is currently an Associate Professor at the Department of Electronics and Communications Engineering, Egypt-Japan University of Science and Technology, Alexandria, Egypt. He received his B.Sc. in Electrical Engineering from Alexandria University, Egypt, and his M.Eng. and Ph.D. from the University of Alberta, Canada. From April 1994 to January 1998, he worked as an instrument engineer with Schlumberger. From May 2000 to September 2001, he was with Murandi Communications Ltd., Calgary, Alberta, where he worked on RF transceivers design. From April 2007 to April 2008, he

worked on RF CMOS transceivers design at Scanimetrics Inc., Edmonton, Alberta. His research interests include the design of RF circuits and systems.

Mohammed Abo-Zahhad received the B.Sc. and M.Sc. degrees in electrical engineering from the University of Assiut, Egypt, in 1979 and 1983, respectively, and the Ph.D. degree from the University of Kent, Canterbury, U.K., and Assiut University (channel system), in 1988. He was a member of the European Society of Circuit Theory and Applications in 1998, a member of the National Communication and Electronics Promotion Committee, and a Reviewer of the National Quality Assurance and Accreditation Authority, NAQQA, Egypt, since 2011. Since 1999, he has been a Professor of electronics and communication engineering with Assiut University. He is currently the Dean of the School of Electronics, Communication and Computer Engineering and has been a Professor of communication and electronics engineering with the Egypt-Japan University of Science and Technology (E-JUST) since 2017. He is also the General Director of the E-JUST Information and Communication Technology Centre. His research interests include biomedical and genomic signal processing, speech processing, optical and digital filters, switched-capacitor, data compression, wavelet-transforms, genetic algorithms, immune algorithms, wireless sensor networks, microwave, millimeter wave wireless communications, energy harvesting, and electronic circuits. He was a recipient of the Encouragement State Award in Engineering, from the Egyptian Research and Technology Academy, Ministry of Higher Education, Egypt, in 2005..